Detection of Water Pipeline Leakages Using High-Resolution Satellite Imagery and Auxiliary Ground Data in Cyprus. Case study of Community Councils of Doros and Monagri.

Christos Theocharidis[1]*[a,b], Christiana Papoutsa[a,b], Kyriacos Themistocleous[a,b], Christodoulos Mettas[a], Diofantos Hadjimitsis[a,b]
[a]ERATOSTHENES Centre of Excellence, Franklin Roosevelt 82, 3012 Limassol, Cyprus.
[b]Cyprus University of Technology, Limassol, Cyprus.

ABSTRACT

Water losses due to pipeline leakages remain a persistent challenge in water-scarce regions, particularly within rural and mountainous communities where detection and maintenance are more complex. On average, 20–30% of distributed freshwater is lost before reaching consumers, and in areas with ageing infrastructure, this proportion can rise to nearly 50%, exacerbating the stress on limited water resources. This study presents a multi-source geospatial approach to detect and verify pipeline leakages in the distribution networks of the Doros and Monagri community councils in Cyprus. The methodology combines analysis of very high- (PlanetScope | 3m) and high- (Sentinel-2 | 10m) spatial resolution satellite data, strategically acquired during prolonged dry periods to maximise the detectability of leakage-induced anomalies in soil moisture and vegetation. Satellite analysis was complemented with drone-based surveys for centimetre-level validation, acoustic noise loggers for in-pipe monitoring, and Ground Penetrating Radar (GPR) profiling to characterise subsurface conditions. The results demonstrate that while some vegetation indices (NDVI, SAVI) were less sensitive to localised leakage signals, moisture-sensitive indices (NMDI, NDWI) consistently highlighted leakage zones. UAV imagery successfully confirmed satellite-detected hotspots, revealing surface manifestations such as cracking and localised greening. Acoustic sensors detected distinct leak-related signals but also produced inconclusive anomalies, with one strong signal most likely originating from pressure-regulating equipment rather than an actual leak. GPR surveys provided critical subsurface validation, with multi-directional profiling reducing false positives and strengthening confidence in anomaly detection. Overall, the integration of satellite, UAV, acoustic, and GPR data proved significantly more effective than any single method, offering a robust and replicable framework for leak detection in semi-arid, rural water networks. The study highlights both the advantages and the limitations of each method and underlines the value of cross-validation for prioritising excavations and maintenance. The findings are directly transferable to other Mediterranean and semi-arid regions facing similar challenges, supporting more efficient, timely, and cost-effective water resource management.

Keywords: Water leakage, PlanetScope, Sentinel-2, Cyprus, GPR, Drones, Acoustic sensors, Google Earth Engine

1. INTRODUCTION

Water pipeline leakages remain a pervasive challenge in water distribution networks worldwide, causing substantial wastage of treated freshwater. On average, 20–30% of distributed water is lost due to leaks before reaching consumers, and in regions with ageing infrastructure, this loss can rise to nearly 50% [1]. In extreme cases, especially in long transmission lines, leakages have been estimated to account for up to 70% of water losses [2]. Such non-revenue water not only represents economic loss but also exacerbates stress on scarce water resources, a critical concern for semi-arid regions in the Mediterranean. Unchecked leaks can also undermine infrastructure (through soil erosion or subsidence) and pose public health risks if pressure drops allow contaminant ingress [3]. This underscores the need for efficient, timely, cost-effective leak detection approaches in water-scarce areas. Various non-invasive techniques have been developed to detect pipeline leaks without excavating or disrupting service. Conventional methods rely heavily on field inspections and sensor measurements along the pipeline. For instance, the exploitation of acoustic leak detection is widely used, where listening devices or correlators pick up the sound of water escaping under pressure, which can indicate leak locations [4–7]. Other techniques include Ground-Penetrating Radar (GPR) to sense soil disturbances or moisture around pipes and

[1] Corresponding author's email: christos.theocharidis@eratosthenes.org.cy

electromagnetic surveys, [8–11]. These traditional approaches, while proven, are often labour-intensive and time-consuming, requiring crews to survey pipelines segment by segment. In remote or mountainous communities, accessing the entire network can be impractical.

Furthermore, their effectiveness may drop in complex terrains or noisy environments. As a result, utilities and researchers have been exploring more efficient monitoring strategies. Remote sensing has emerged as a powerful non-invasive approach to complement ground methods for leak detection. Observing the surface indicators from above offers wide-area coverage that can be especially valuable in rural or hard-to-access areas. The leaked water increases soil moisture and often leads to abnormal vegetation growth near a leak, particularly in dry climates where such green patches stand out clearly [12,13]. Recent advances in satellite technology now provide very high-resolution imagery, enabling the detection of even minor leak-induced effects. Researchers have leveraged very high-resolution imagery alongside field spectroscopy and GIS to detect water pipeline leaks. In particular, Agapiou et al (2013) [14] demonstrated that remote sensing could identify anomalies in vegetation greening and surface temperature patterns around leak locations, where enhanced moisture leaks triggered visible greening in otherwise dry landscapes. Moreover, they performed a multi-temporal satellite analysis comparing images before and after suspected leak events or across seasons, distinguishing leak-induced greening from normal season variation. A key consideration in such studies is image timing. Acquiring imagery during prolonged dry periods significantly improves detection, since any observed moist soil or vigorous vegetation is more likely due to a leak than recent rainfall. Moreover, the spatial resolution of the sensor is critical, where small leaks affect only a localised area, so satellites with finer pixels can capture these small wet patches more distinctly. Where satellite resolution or revisit frequency is a limitation, drones or Unmanned Aerial Vehicle (UAV) deployments offer a flexible complement. Drones can fly low and carry high-resolution cameras or thermal sensors to investigate suspected leak areas in detail [15]. Drones thus bridge the scale gap by providing on-demand, high-detail observations to validate satellite-detected hotspots.

Beyond optical and thermal techniques, researchers are now investigating microwave radar sensors for leak detection. Synthetic Aperture Radar (SAR) satellites like Sentinel-1 can penetrate cloud cover and are sensitive to soil moisture [16]. While historically SAR has seen limited application for water pipeline leaks, recent studies made their presence starting to use SAR sensors for water leakage detection with high success [17–19]. Moreover, the radar provides moisture-sensitive features that complement the optical indicators of vegetation and temperature, improving detection accuracy in environments where vegetation response alone might be insufficient, such as leaks under paved surfaces or sparse vegetation. Mediterranean regions such as Cyprus offer an ideal testing ground for remote sensing-based leak detection, where numerous studies have been conducted [20–22], as its semi-arid climate is characterised by long, dry summers and minimal rainfall, creating a strong contrast between leak-induced anomalies and the surrounding environment. Therefore, the lack of extended rainfall creates a controlled background against which leaks are easier to detect.

In this context, the present study aims to demonstrate the effectiveness of integrating very high-resolution satellite imagery, drone observation, and ground-based inspections to detect water pipeline leakages in rural, semi-arid environments. Focusing on the Doros and Monagri community councils in Cyprus, the approach combines PlanetScope and Sentinel-2 imagery acquired after a prolonged dry period with drone-based surveys for accurate mapping purposes and GPR measurements along a selected road segment within the study area.

2. STUDY AREA

The study area focuses on the community councils of Doros and Monagri villages, located in the Limassol district of Cyprus (Figure 1). This rural, mountainous region lies within the Troodos foothills and is characterised by a mosaic of agricultural land, shrubland, and forested slopes. The area's semi-arid Mediterranean climate features hot, dry summers and mild, wet winters, making water management a critical challenge. The local water distribution network is supplied through three main storage facilities, the Doros, the Monagri and the St. Seryios water tanks, with additional tanks serving both Doros and Monagri. The network spans complex terrain, including narrow valleys and steep inclines, complicating maintenance and leak detection operations. The boundaries of the two community councils, as shown in yellow on the map, define the spatial extent of the investigation.

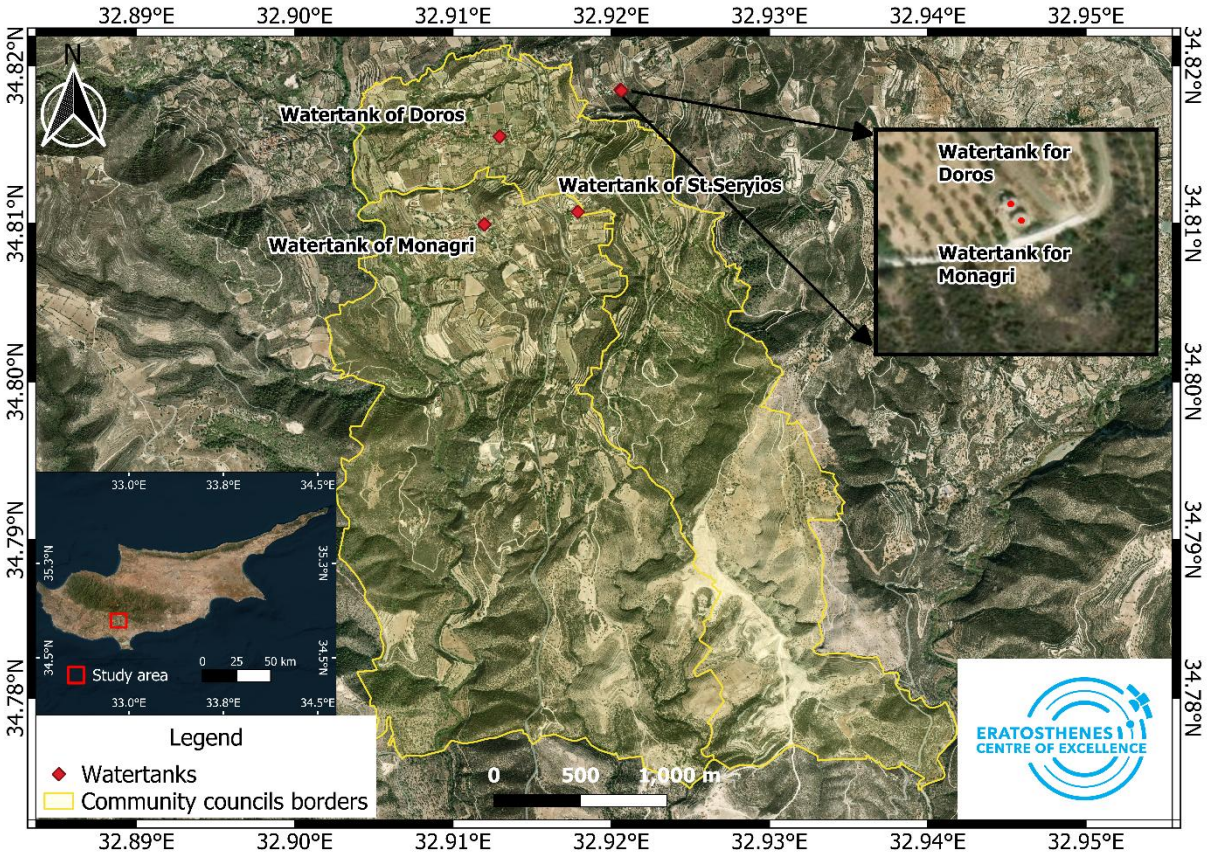

Figure 1. The spatial extent of the study area covers the Doros and Monagri community councils in Cyprus.

3. DATA AND METHODOLOGY

3.1 CHIRPS satellite data

The selection of the satellite data was designed to optimise the detection of the surface anomalies caused by leaks, such as increased soil moisture under the prevailing dry conditions of the study area. To ensure that any detected moisture anomalies were attributable to potential pipeline leakages rather than recent precipitation, the selection of satellite imagery was guided by rainfall data from the Climate Hazards Group Infrared Precipitation with Station data (CHIRPS) dataset. CHIRPS provides quasi-global daily precipitation estimates by integrating satellite observations with in-situ measurements from meteorological stations [23]. Analysing CHIRPS data for the study area, periods of extended drought with zero recorded rainfall were identified. These rain-free intervals formed the basis for further selecting the satellite data, ensuring that the observed anomalies were more likely linked to potential leakage events rather than natural weather patterns.

3.2 Sentinel-2 satellite data

In total, 11 images from Sentinel-2 level-2A (10m spatial resolution) surface reflectance products were acquired between 26 June and 22 August 2024 (5 images); 05 July and 30 July 2025 (6 images) with <10% cloud coverage. Image pre-processing and analysis were conducted within the Google Earth Engine (GEE) environment[24]. Sentinel-2's multispectral capabilities allowed for detailed moisture assessment across the study area, calculating the Normalised Difference Moisture Index (NDMI) and the Normalised Multi-band Drought Index (NMDI) as follows:

$$NDMI = \frac{NIR - SWIR1}{NIR + SWIR1} \quad (1)$$

$$NMDI = \frac{NIR - (SWIR1 - SWIR2)}{NIR + (SWIR1 - SWIR2)} \quad (2)$$

where *NIR* (B8) is the Near-Infrared band / Band 8 of Sentinel-2, *SWIR1* (B11) and *SWIR*2 (B12) are the Short-Wave Infrared bands / Bands 11 and 12 of Sentinel-2. The NDMI was primarily used to detect vegetation and soil moisture variations along the known pipeline corridors. Higher NDMI values indicate greater water content, with values above approximately 0.2 typically signifying moist vegetation or soil, and lower values indicating dry conditions[25]. Furthermore, highlighting areas with increased water content during the prolonged dry season, NDMI helped identify localised moisture anomalies that could be linked to leakage events rather than natural hydrological processes. On the other hand, the NMDI was employed to enhance drought condition monitoring and to differentiate genuine leak-induced moisture from residual soil wetness or vegetation unrelated to leaks. For NMDI, values approaching 0.25 or higher generally indicate higher moisture content in either vegetation or bare soil, whereas negative or near-zero values are typical of dry surfaces [26].

3.3 PlanetScope satellite data

Very high-resolution imagery (3m spatial resolution) from the PlanetScope Dove satellites was obtained through the Planet Insights platform [27]. A total of 38 PlanetScope images were acquired between 1 July and 20 August 2024, covering the same dry season period as the Sentinel-2 data. Image pre-processing and analysis were performed in ArcGIS Pro (v.3.5), enabling high-precision mapping and visual interpretation of potential leak-related anomalies. The four spectral bands of PlanetScope (Blue, Green, Red, NIR) allowed the calculation of three vegetation and moisture indices suitable for detecting anomalies. The Normalised Difference Vegetation Index (NDVI) was used to assess vegetation vigour and canopy density, with unexpectedly high values during the dry season along pipeline routes potentially indicating localised moisture from leakage. The Normalised Difference Water Index (NDWI) was applied to highlight water content in vegetation and soil by contrasting green and NIR reflectance, thus enhancing the identification of possible moist areas and wet patches in otherwise dry surroundings. In addition, the Soil Adjusted Vegetation Index (SAVI), which introduces a soil brightness correction factor, was employed to improve vegetation detection in areas with sparse cover where soil reflectance could otherwise mask subtle greening caused by leaks.

PlanetScope imagery acquired in four spectral bands (Blue, Green, Red, Near-Infrared) was used to compute the following indices:

$$NDVI = \frac{(NIR - RED)}{(NIR + RED)} \quad (3)$$

$$NDWI = \frac{(GREEN - NIR)}{(GREEN + NIR)} \quad (4)$$

$$SAVI = \frac{\big((NIR - RED) \times (1 + L)\big)}{(NIR + RED + L)} \quad (5)$$

Where L = 0.5, reducing soil brightness influence in areas with sparse vegetation.

To enhance the detection of abnormal moisture or vegetation signals that could indicate leak-related anomalies, all indices (NDMI, NMDI, NDVI, NDWI, SAVI) were further standardised by computing their Z-scores. This statistical transformation allowed each pixel value to be expressed relative to the mean and standard deviation of the reference time series, highlighting deviations from the typical seasonal conditions. Positive Z-scores indicated anomalously high moisture

or greenness compared to the background conditions, whereas negative Z-scores indicated abnormally low values. Different reference statistics (minimum, maximum, and median) were tested to identify the most reliable anomaly representation. The median-based Z-score proved most effective for Sentinel-2, as it suppressed outliers and provided a stable background reference, while the maximum-based Z-score was more suitable for PlanetScope due to its higher spatial resolution and greater sensitivity to short-term vegetation and moisture peaks. This tailored approach ensured anomalies were consistently and robustly highlighted in both datasets. To further reduce misinterpretation from unrelated features, the pixel selection process was carried out manually through visual inspection of the anomaly maps, focusing only on pixels located along the pipeline route and within dry fields and vegetation to more clearly distinguish potential anomalies. Non-relevant features such as tree canopies, buildings or paved roads were systematically excluded after a complete inspection of the pipeline network. This combined statistical and visual filtering ensured that only meaningful anomalies related to possible leak-induced moisture were retained for further analysis.

3.4 Acoustic sensors

Acoustic sensing technology was deployed to monitor the water distribution pipelines in the study area directly and complement satellite-based analysis. A total of 10 acoustic sensors were installed in Doros village, and eight acoustic sensors in Monagri, placed along the main pipeline network (Figure 2 and Figure 3). The installation points were selected in consultation with the local community authorities, who provided critical knowledge on the pipeline layout and locations most susceptible to potential leakage. The sensors, provided by VonRoll Hydro, were of the type Ortomat-MT correlating noise loggers and were integrated into the Infraport monitoring system, which enables real-time data acquisition and remote supervision (Figure 4). For optimal performance, the acoustic sensors in Doros were synchronised at a frequency of 96.8 MHz, while those in Monagri were synchronised at 106 MHz, ensuring accurate signal transmission and correlation across the network. Synchronisation at fixed frequencies ensures that all loggers operate on a common reference, improving the accuracy of cross-correlation analysis used to determine leak locations. It also minimises potential signal interference and enhances the ability to distinguish true leak-generated noise from background acoustic variability, thereby increasing the reliability of leak detection.

Acoustic leak detection works on the principle that water escaping under pressure generates a distinct acoustic signal, where the turbulence and vibration at the leakage point cause a high-frequency noise. The intensity and frequency of this signal can be detected by correlating sensors placed at intervals along the pipeline. By comparing the time and strength of the signal received, the approximate location of the leak can be triangulated. This method has been widely used in water distribution systems globally due to its ability to identify leaks without excavation [28–30].

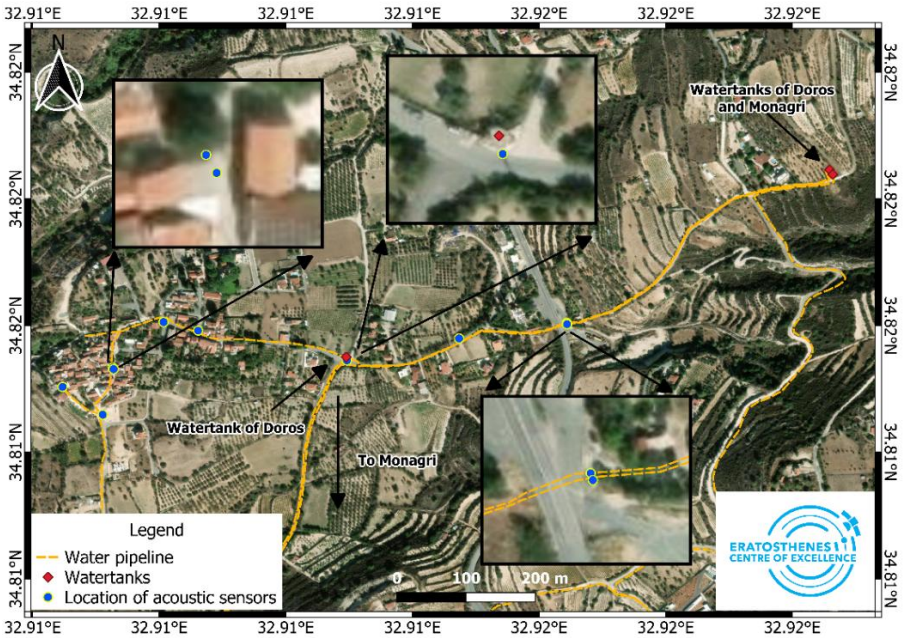

Figure 2. Represents the study area of Doros village, where the yellow line indicates the water distribution network; the red squares indicate the watertanks, and the blue dots indicate the location where the acoustic sensors were installed.

Figure 3. Represents the study area of Monagri village, where the yellow line indicates the water distribution network; the red squares indicate the watertanks, and the blue dots indicate the location where the acoustic sensors were installed.

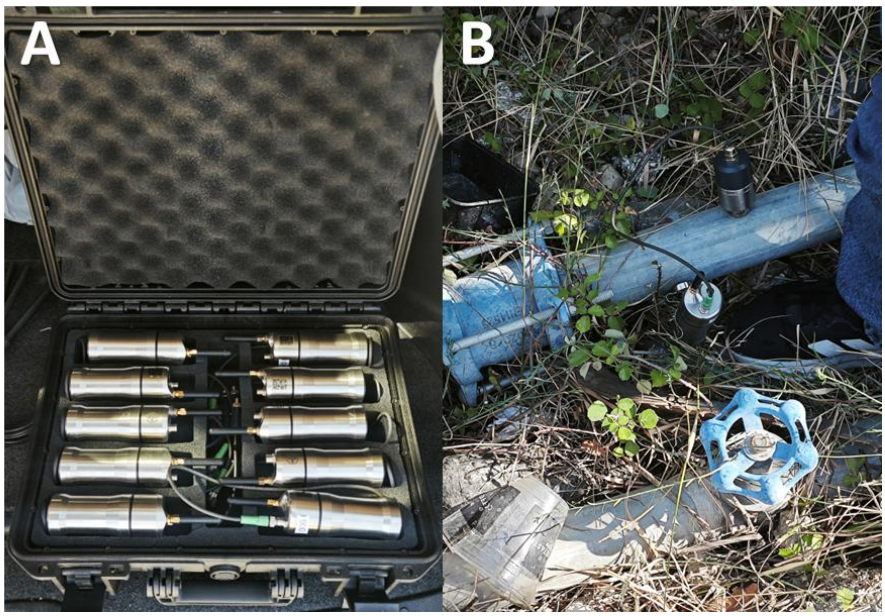

Figure 4. A) Acoustic sensors used for pipeline monitoring – VonRoll Hydro *Ortomat-MT* correlating noise loggers; B) Field installation of the sensors on a water distribution pipeline (Image captured on 02 July 2025).

3.5 Ground Penetrating Radar measurements

To further support the satellite and acoustic sensor analyses, GPR was employed along a selected road segment in Doros village to investigate the subsurface conditions of the pipeline directly. GPR is a non-invasive geophysical technique that transmits electromagnetic waves into the ground and records the reflected signal generated by subsurface structures,

changes in material properties, or anomalies such as voids and zones of increased moisture [31]. When water leaks occur from buried pipes, the leaked water alters the dielectric properties of the surrounding soil, creating reflection patterns that can be detected in GPR profiles [32]. Ground-penetrating radar (GPR) is effective for detecting water leakage in buried utilities because it responds to contrasts in dielectric properties. Saturated soil around a leak produces amplitude and frequency shifts relative to the dry surroundings, often disrupting the clean hyperbolas expected from intact pipes. These diagnostic changes make GPR a strong complement or alternative to acoustic methods, especially for non-metallic pipelines commonly used in distribution networks.

This study used a MALA Easy Locator system equipped with a shielded 500 MHz antenna, mounted on a four-wheel cart to facilitate smooth acquisition over paved and unpaved surfaces (Figure 5). The system was connected to a GPS receiver for precise georeferencing of the profiles. The acquisition settings were optimised to balance depth penetration and resolution; a time window of approximately 78 ns (corresponding to ~4 m penetration depth in dry soils) was selected, with a sampling frequency of 7549 MHz and a trace interval of 0.04 m. These parameters were chosen to provide sufficient depth coverage to encompass the buried pipeline while maintaining a high level of detail in the radargrams.

The survey design followed a systematic strategy to maximise coverage and ensure redundancy for anomaly verification. As shown in Figure 6, the GPR survey was conducted along the pipeline route between point A (elevation 486 m) and point B (elevation 502.5 m). The survey targeted a potable water main running along the primary road where leakage was suspected. Parallel and cross-line acquisition geometry was adopted to (i) resolve pipe position and depth through hyperbola apex picking along the alignment and (ii) confirm potential anomalies across the alignment where leakage plumes may spread laterally through permeable backfill. Previous work highlights that combining orientations improves utility detection and localisation in traffic corridors. Data collection was performed reciprocally, beginning at point A, moving towards point B, and returning along the same path. The process was repeated nine times in total, deriving nine profiles of the road in the end. The bidirectional acquisition strategy helped reduce directional bias, ensured consistency of detected features, and improved confidence in identifying persistent anomalies. To further constrain the lateral extent of potential leakage zones, parallel to the road transects (profiles P1–P9) were acquired across the road surface (Figure 7). Together, the longitudinal and perpendicular profiles created a dense grid of measurements, improving the spatial coverage of the survey and allowing a more robust interpretation of subsurface anomalies potentially related to leakage.

A total of 21 perpendicular survey lines were acquired across the study area (Figure 8). These tie-lines were critical in validating the anomalies observed on parallel profiles. They revealed the lateral spread of high-amplitude patches along trench backfill and confirmed hyperbola distortions at specific chainages. Using multiple cross-lines improved confidence in anomaly location and reduced the chance of false positives, which aligns with previous recommendations for utility detection in road corridors. During acquisition, live monitoring of the radargram of the MALA XV monitor allowed immediate inspection of signal quality and detection of any strong reflectors or hyperbolic signatures. The presence of hyperbolas in the radargrams was particularly interesting, as they can indicate buried utilities, junctions, or anomalies related to localised soil disturbance and moisture accumulation near leakage points.

Data processing followed a standard workflow: time-zero correction, dewow with trace-mean removal, broad band-pass filtering, time-variant gain, background removal, and time-to-depth conversion. Envelope extraction was then used to highlight amplitude anomalies, and f-k migration was applied to sharpen blurred signatures and collapse diffractions where saturated soils masked the pipe response.

Potential leakage was interpreted from multiple criteria, including disruption or attenuation of the pipe hyperbola compared with adjacent segments, compact amplitude anomalies in the envelope forming coherent patches aligned with the trench, localised reduction of dominant frequency, and lowered EM velocity derived from hyperbola fitting in suspect zones. These signatures are consistent with the reported effects of water-saturated soils on GPR responses and differences observed across soil types and pavement conditions. For example, measured velocities are lower in fine-grained or wet soils than under concrete pavements reinforced with iron mesh, which adds further contrast.

The water pipe was consistently tracked along the road at depths of approximately 4 m. Parallel profiles showed clear hyperbola apexes, with cross-lines confirming intersections. The average EM velocity for intact sections was ~0.10 m/ns, consistent with the local soil subgrade. Where potential leakage occurred, hyperbola disruption and bright envelope patches were observed, meeting the multi-criteria threshold for anomaly classification.

Integrating GPR into the overall methodology provided an essential Ground-based diagnostic tool. While satellite imagery and vegetation indices pointed to surface anomalies and acoustic sensors captured leak-generated noise within the pipe, GPR offered a subsurface perspective, capable of directly imaging the soil-pipeline interface. This combination of perspectives increased the robustness of the leak detection framework, ensuring that candidate leakage zones could be investigated with higher precision.

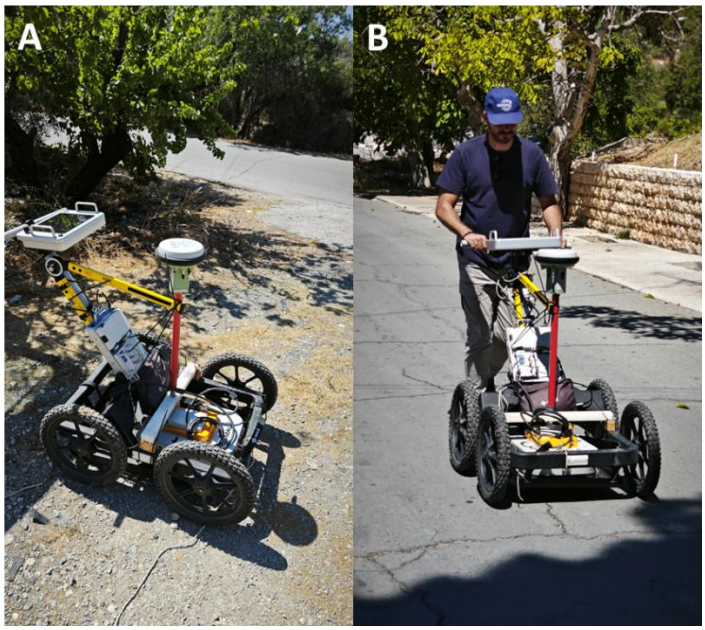

Figure 5. A) MALA GPR, which was used in this study; B) During the GPR measurement (Images captured on 04 July 2025).

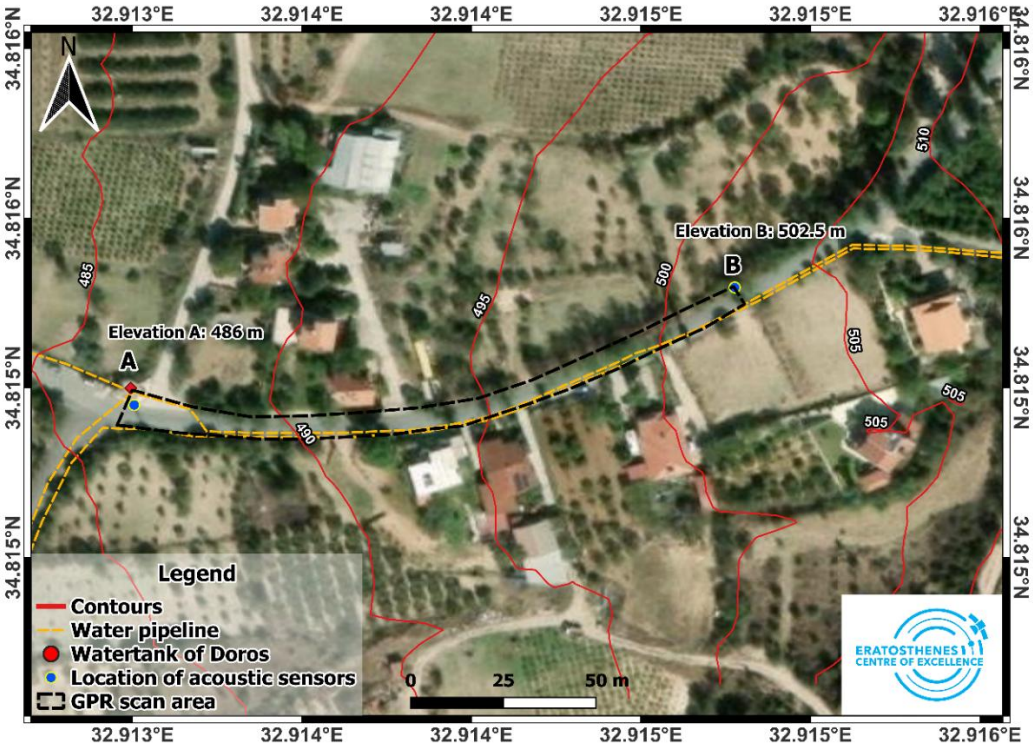

Figure 6. The GPR survey carried out on a selected road in Doros village.

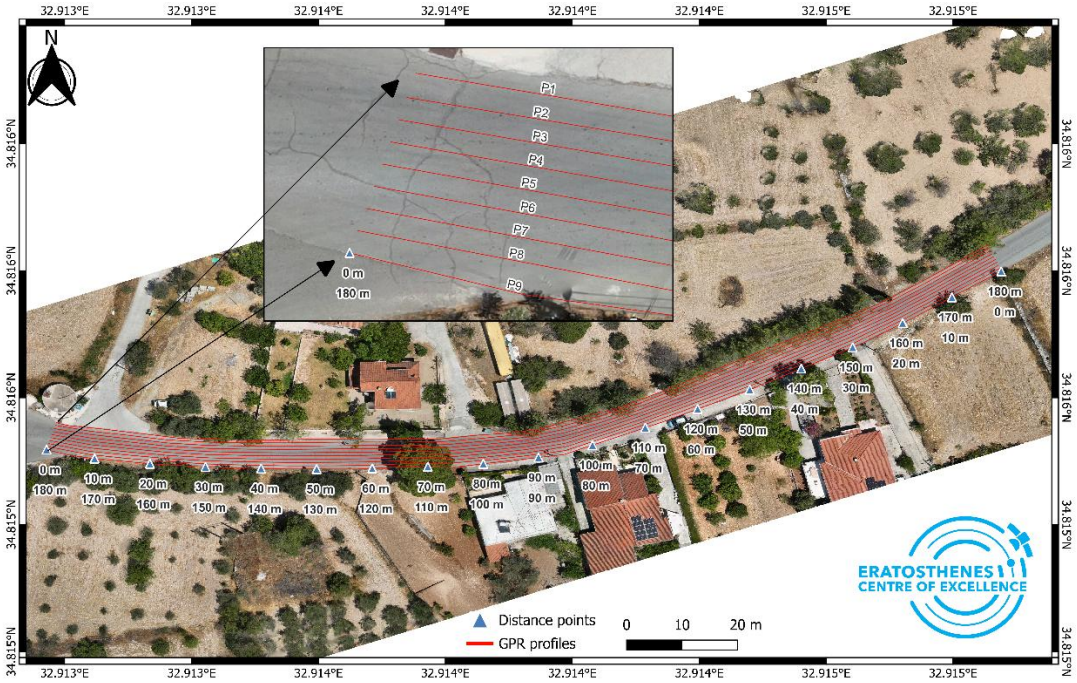

Figure 7. Survey map of the GPR measurements in Doros village (Drone image captured on 04 July 2025). Red lines indicate the locations where the GPR profiles were acquired during the field campaign (horizontal / across the road).

Figure 8. Survey map of GPR measurements in Doros village. Black lines indicate the locations where the GPR profiles were acquired during the field campaign (vertical towards the road) (Drone image captured on 04 July 2025).

3.6 Drone imagery

To complement the Ground-based geophysical surveys and ensure a precise spatial framework for interpreting GPR measurements, a UAV mapping campaign was carried out using a DJI Mavic 3 drone (Figure 9). The flights were designed to cover both the road segment where the GPR surveys were conducted in Doros and the connecting road leading towards Monagri village (Figure 11A). The UAV survey provided a detailed orthophotomosaic by acquiring very high-resolution imagery with a Ground Sampling Distance (GSD) of 0.1 m. The drone was flown in automated grid missions to ensure systematic coverage and high forward and side overlap, which are essential for robust photogrammetric processing. These images were later processed using structure-from-motion (SfM) photogrammetry, generating a seamless georeferenced orthomosaic. This product was then integrated into a GIS environment to serve as the base map for aligning GPR transects, acoustic sensor locations, and field observations. The advantage of this approach lies in its ability to provide a centimetre-

level visual context of the survey area, capturing both the surface conditions of the road and its surrounding environment. This not only facilitated the precise positioning of geophysical measurements but also ensured reproducibility of the results by documenting the exact layout of the survey area at the time of data collection.

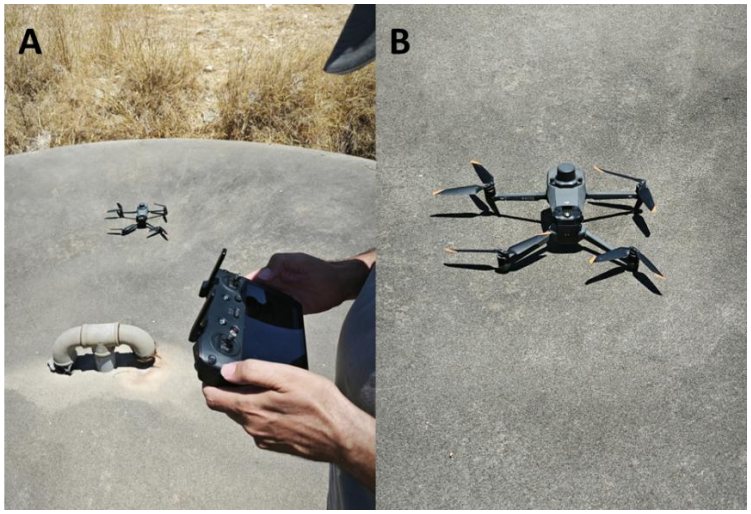

Figure 9. A) Drone pilot operating the UAV during take-off near the survey site; B) Close-up of the DJI Mavic 3 drone on the ground before flight.

4. RESULTS

4.1 Satellite and drone images

The combined use of satellite imagery, acoustic sensors, GPR measurements and UAV mapping provided multiple evidence of leakages along the pipeline in different spots. In the first case (Figure 10A), a persistent low-intensity leakage was identified near the Doros water tank, where water had been seeping continuously for several months. This prolonged loss created a distinct patch of greenery that remained visible even during extended drought periods. Sentinel-2 imagery confirmed the presence of the anomaly (Figure 10) between 26 June and 22 August 2024 using the NDMI, while PlanetScope imagery also detected the signal between 1 July and 20 August 2024 through the NDWI (Figure 10C). Field inspection was conducted approximately one year later during the project, verifying the leakage and repairing the damage. At that time, a smart meter was installed on the site to enable continuous monitoring and prevent similar undetected losses. The second case involved another leakage located only a short distance from the Doros water tank. Here, cracks on the road surface and strong early-morning humidity patterns provided critical indicators of water loss. Sentinel-2 captured the anomaly through the NDMI at approximately 08:30 local time, when the low solar angle allowed surface moisture to remain detectable before evaporation occurred. By contrast, PlanetScope acquisitions at midday did not capture the anomaly, as higher solar radiation had already dried the surface, masking the signature of moisture. UAV imagery (Figure 11) also corroborated the satellite findings, showing clear signs of road cracking and patches of unjustified greenness consistent with localised soil moisture linked to leakage. Subsequent excavation at the site confirmed the presence of a fractured pipeline, which was repaired by the local authorities (Figure 10B).

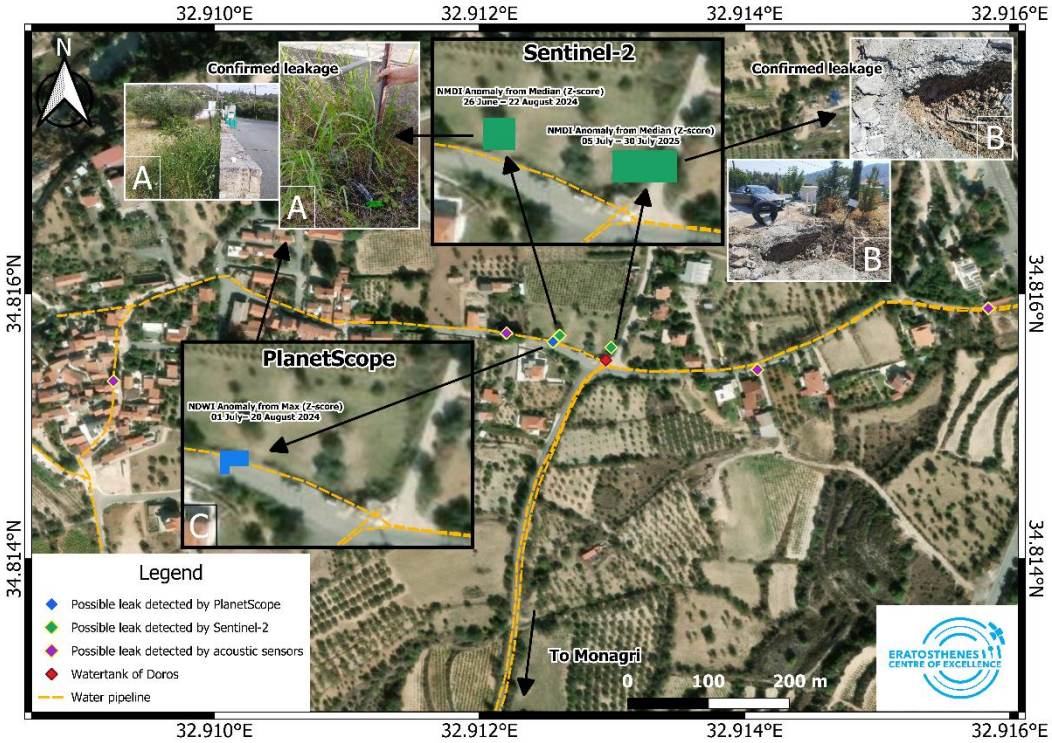

Figure 10. Leakages detected from Sentinel-2, PlanetScope and acoustic sensors. A) Leakage was detected from Sentinel-2, approximately 27m to the left of the Doros village water tank. B) Leakage detected 7m north of the Doros village water tank. C) The same leakage as "A" was also detected from PlanetScope imagery.

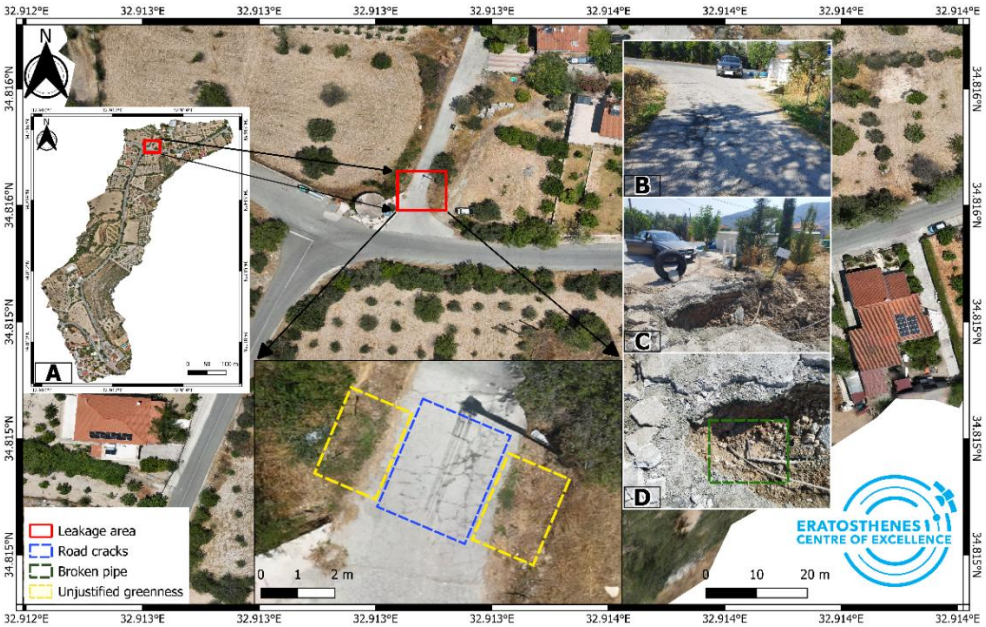

Figure 11. Leakage mapped from drone imagery. A) UAV orthomosaic; B) Road surface with visible cracks and early signs of moisture stress; C) Excavation works conducted by local authorities revealing the leakage site; D) Broken pipeline section exposed during excavation, confirming the source of water loss.

4.2 Acoustic sensors

In Doros, ten Ortomat MT acoustic sensors (Figure 4A) were deployed along the main pipeline, with the network covering the section between the Doros water tank and the adjacent distribution lines. The analysis revealed four potential leakage anomalies, but only one, located between points A and B (Figure 12), was considered significant enough to investigate further. The correlation analysis between the two sensors showed a distinct peak, strongly indicative of a leak signal along this section of the pipeline. Moreover, the raw acoustic recordings from both positions capture a persistent and unusual noise, which may acoustically resemble the signature of water escaping under pressure. This abnormal sound was spatially consistent with the correlation peak, strengthening confidence in detecting a genuine leakage at this location.
Regarding the remaining three anomalies, two were located within the village core, while the third was outside the village (Figure 10). Although the sensors acquire data during the quietest hours of the night (around 04:30 a.m.) when water demand is minimal and the distribution network is expected to be hydraulically calm, interference was still present. Specifically, mechanical equipment regulating water pressure, such as pressure-reducing valves, generated parasitic hydraulic noise that masked or distorted the correlation signals. While the overall village environment was quiet, these artificial noise sources undermined the results' clarity. Since these anomalies were not corroborated by Sentinel-2 or PlanetScope indices, drone imagery or GPR measurements, they were ultimately considered inconclusive.
In Monagri, eight acoustic sensors were deployed along the pipeline network (Figure 3). Despite being left in place for approximately three weeks, the system did not identify any major leakage events. Several factors may have contributed to this absence of detections. First, the network layout in Monagri is highly complex, with narrow streets and limited accessible points for sensor placement, resulting in a relatively sparse sensor configuration. Second, the physical constraints of the village reduced the ability to establish optimal sensor spacing, which is critical for reliable correlation. Third, no significant water losses may have occurred during the monitoring period. These factors likely explain why no significant leak signatures were detected. Although no positive detections were made, this outcome is nonetheless informative since it highlights both the challenges of deploying acoustic methods in dense village environments and the importance of complementary techniques such as satellite and drone-based monitoring.

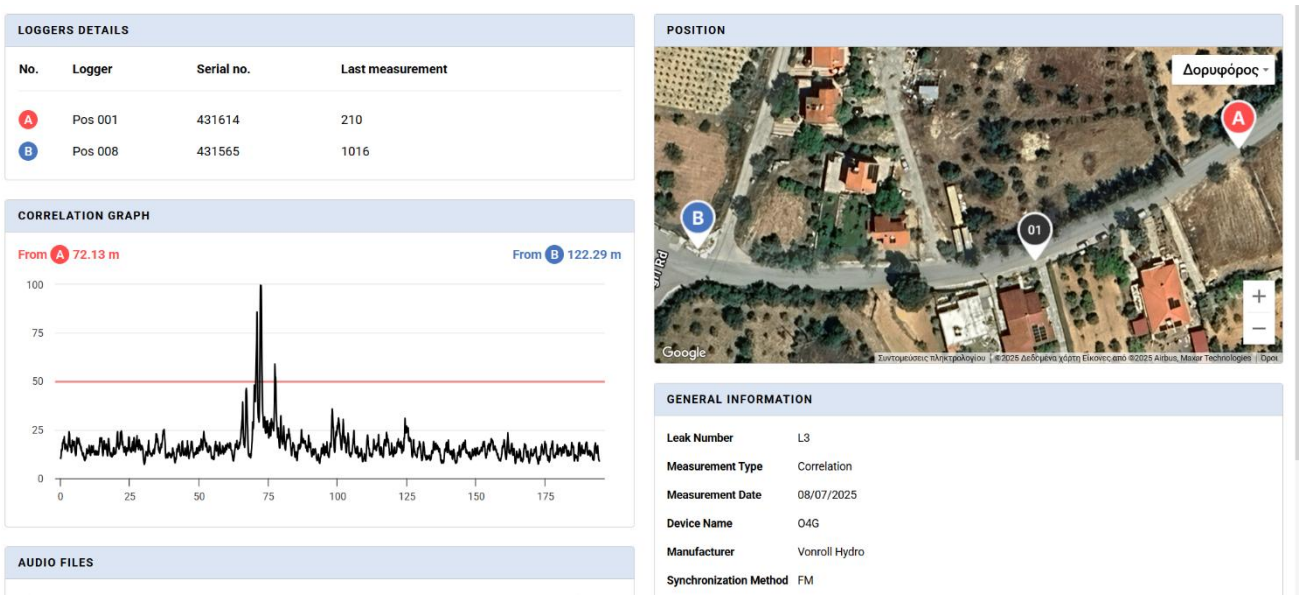

Figure 12. A screenshot from Infraport shows the logger's details, the correlation graph, and the position of the two acoustic sensors with the potential leakage point.

4.3 GPR measurements

The potable water pipe was traced along the primary road corridor in Monagri and Doros at an average depth of ~4 m. Parallel profiles provided continuous hyperbola apexes marking the pipe axis, while cross-lines confirmed the pipe positions and depth picks at regular intervals. The average EM velocity derived from intact segments was ~0.10 m/ns, consistent with the soil subgrade. Several segments along the mapped pipe alignment displayed GPR characteristics consistent with leakage. These anomalies were identified when at least two predefined criteria were present: hyperbola

disruption, bright amplitude patches in the envelope, frequency reduction, or local velocity drop (Figure 13). GPR surveys can successfully detect underground utilities, with buried pipes typically appearing as distinct hyperbolas in radargrams. The hyperbolic response arises from the strong dielectric contrast between the pipe material and the surrounding soil. The shape and scale of the hyperbola depend on pipe dimensions: larger pipes generate wider hyperbolas, while smaller pipes produce narrower ones. In cross-section, the hyperbola's upper arc approximates a semicircle's perimeter corresponding to the pipe diameter.

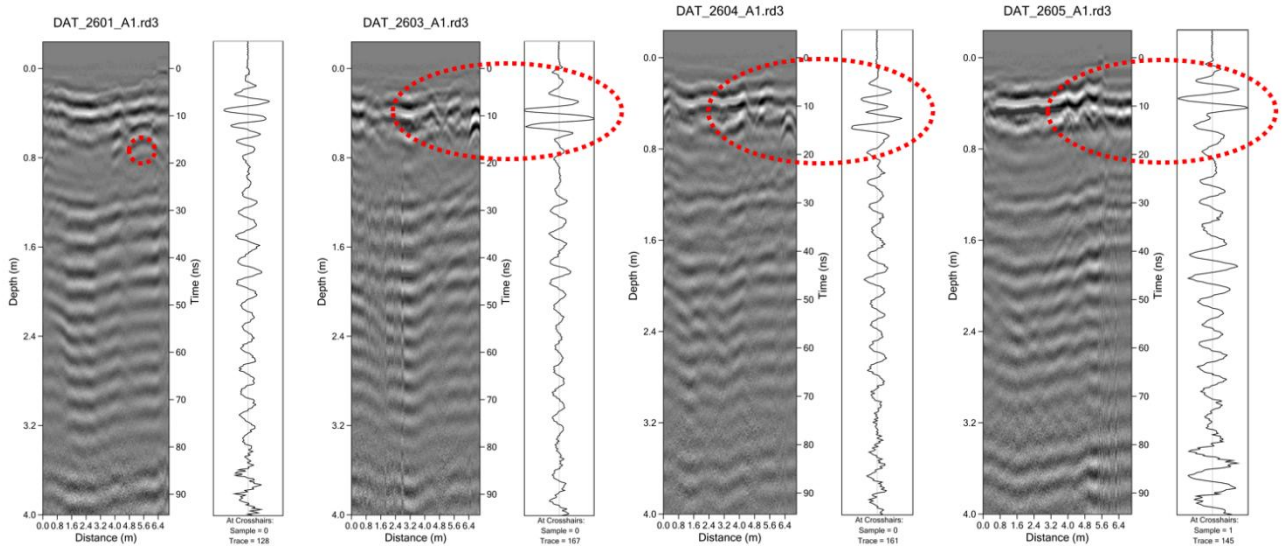

Figure 13 presents representative traces and radar sections from selected profiles within the study area. In profile DAT_2021, the water pipe is clearly visible as a well-defined hyperbola, consistent with an intact pipe segment. By contrast, profiles DAT_2603, DAT_2604, and DAT_2505 exhibit distorted or attenuated hyperbolas accompanied by localised amplitude anomalies. These signatures are consistent with probable leakage, where surrounding soil saturation modifies the dielectric properties and introduces additional scattering features adjacent to the pipe. The comparison highlights the contrast between intact and anomalous responses, underscoring the diagnostic value of hyperbola morphology and amplitude behaviour in leakage detection.

By contrast, the surveys along profiles DAT_2607 - DAT_2614 did not reveal clear leakage-related anomalies. The absence of diagnostic hyperbolas or amplitude patches in these sections is attributed to an iron mesh embedded in the concrete pavement above the water line. Reinforced concrete strongly attenuates and scatters the radar signal, masking the pipe response and obscuring potential leak signatures. This limitation is consistent with findings that metallic reinforcement in pavements reduces GPR penetration and limits the ability of utility detection.

5. DISCUSSION

The results of this study highlight both the potentials and the limitations of using multi-source geospatial approaches for water leakage detection in semi-arid rural environments. Although several vegetation and moisture indices were tested in this study (NDVI, SAVI, NDWI, NDMI, NDMI), not all yielded consistent results across the confirmed leakage sites. For example, NDVI and SAVI, which are highly effective for assessing general vegetation vigor, did not provide reliable indications of localised leaks, as they are more sensitive to overall canopy density and photosynthetic activity rather than subtle soil moisture changes. Similarly, NDMI showed weaker responses than NMDI in this case, particularly under dry-season conditions where sparse vegetation and soil signals dominated. Nevertheless, applying multiple indices was essential for ensuring methodological robustness, as it allowed us to confirm that the detected anomalies were not artefacts of a single index. This comparative approach demonstrated that while some indices are less effective for pinpointing small-scale leakage in semi-arid environments, they provided a necessary control that increased the confidence in anomalies highlighted by the more responsive indices (NMDI and NDWI).

Integrating UAV imagery was pivotal in bridging the spatial and temporal gap between satellite observations and field verification. High-resolution orthomosaics provided centimetre-level context for interpreting spectral anomalies and allowed visual confirmation of surface manifestations such as road cracking, moisture patches, or abnormal greening. This capability proved particularly valuable in cases where diurnal variation masked satellite-detected anomalies—such as morning moisture visible in Sentinel-2 imagery but absent in midday PlanetScope acquisitions.

Acoustic sensing offered complementary subsurface evidence but illustrated inherent challenges in complex village environments. While the system successfully identified strong correlation peaks associated with genuine leaks in Doros, additional anomalies detected in Doros and Monagri were ultimately deemed inconclusive. Importantly, in Doros, one of the strongest inconclusive signals was located near pressure-regulating equipment, and there is a high probability that the anomaly originated from hydraulic noise generated by this device rather than from a real leakage. This highlights a critical limitation of acoustic approaches in built networks, where parasitic signals from infrastructure elements can mask or distort actual leak signatures. These findings emphasise that acoustic detection alone is insufficient and should be integrated with remote sensing and Ground-based methods to minimise false alarms.

Ground Penetrating Radar (GPR) provided an essential subsurface diagnostic perspective, enabling direct imaging of the soil–pipeline interface. The inclusion of 21 vertical profiles significantly strengthened the interpretation. These cross-lines confirmed the lateral extent of anomalies and distinguished genuine leak signatures from isolated noise or processing effects. This approach follows established recommendations that multi-directional profiling increases detection reliability, especially in road corridors where traffic-related subsurface disturbances complicate interpretation. The anomalies identified in both Monagri and Doros consistently displayed the expected leakage signatures: attenuation of hyperbolas in raw data, restoration of pipe position after migration, bright amplitude patches in the envelope, and measurable velocity reductions. This convergence of evidence across multiple lines and orientations supports classifying at least one area as a probable leakage zone. The multi-sensor framework adopted in this study demonstrated clear advantages over single-method approaches. Each technology contributed complementary information: satellite indices provided wide-area coverage and temporal monitoring, UAV imagery delivered fine-scale validation, acoustic sensors offered in-pipe evidence, and GPR supplied subsurface confirmation. Converging evidence across these independent methods was key to discriminating genuine leakage from noise or unrelated anomalies.

The study also revealed practical insights for rural communities with limited monitoring capacity. Firstly, the strategic timing of satellite acquisitions during prolonged drought proved critical, as it amplified the contrast between leakage-induced anomalies and the dry background. Secondly, deploying acoustic sensors in sparsely accessible networks requires careful planning of spacing and synchronisation to avoid inconclusive results. Finally, cross-validation through UAV and GPR ensures that limited financial and human resources are invested in excavations only at sites with high confidence of leakage. Overall, the findings reinforce that no single method can reliably detect water leakages in complex rural distribution networks. Instead, a multi-source, cross-validated approach maximises detection accuracy, reduces false positives, and provides actionable intelligence for water utilities. Other community councils in Cyprus and similar semi-arid regions can replicate this integrated framework, enabling more effective and timely water resource management.

ACKNOWLEDGEMENTS

The authors acknowledge the WATERLEAKS: “Use of non-invasive technologies to detect water losses in water supply networks” Project which is funded by the Cyprus Rural Development Programme 2014 – 2020 (Measure 19, Scheme 19.2.4 “Cooperation Actions”) under the LEADER Community Initiative through the Development Agency of Lemesos. Also, the authors acknowledge the 'EXCELSIOR': ERATOSTHENES: Excellence Research Centre for Earth Surveillance and Space-Based Monitoring of the Environment H2020 Widespread Teaming project (www.excelsior2020.eu). The 'EXCELSIOR' project has received funding from the European Union's Horizon 2020 research and innovation programme under Grant Agreement No 857510, from the Government of the Republic of Cyprus through the Directorate General for the European Programmes, Coordination and Development and the Cyprus University of Technology.

REFERENCES

[1] Farah, E. and Shahrour, I., "Water Leak Detection: A Comprehensive Review of Methods, Challenges, and Future Directions," Water **16**(20), 2975 (2024).

[2] Al Hassani, R., Ali, T., Mortula, M. M. and Gawai, R., "An Integrated Approach to Leak Detection in Water Distribution Networks (WDNs) Using GIS and Remote Sensing," Appl. Sci. **13**(18), 10416 (2023).

[3] O'Keeffe, J., "Water storage and emerging challenges in a changing climate," Ottawa Natl. Collab. Cent. Environ. Heal. (2024).

[4] Müller, R., Illium, S., Ritz, F., Schröder, T., Platschek, C., Ochs, J. and Linnhoff-Popien, C., "Acoustic leak detection in water networks," arXiv Prepr. arXiv2012.06280 (2020).

[5] Awwad, A., Yahyia, M., Albasha, L., Mortula, M. M. and Ali, T., "Communication network for ultrasonic acoustic water leakage detectors," IEEE Access **8**, 29954–29964 (2020).

[6] Gao, Y., Brennan, M., Joseph, P. F., Muggleton, J. M. and Hunaidi, O., "On the selection of acoustic/vibration sensors for leak detection in plastic water pipes," J. Sound Vib. **283**(3–5), 927–941 (2005).

[7] Cody, R., "Acoustic Monitoring for Leaks in Water Distribution Networks" (2020).

[8] Meng, X., Huang, Z., Deng, X., Liu, H., Fang, H., Liu, C., Zhang, X. and Cui, J., "Leakage detection and localisation of buried water pipe using ground penetrating radar," Measurement, 117902 (2025).

[9] Nakhkash, M. and Mahmood-Zadeh, M. R., "Water leak detection using ground penetrating radar," Proc. Tenth Int. Conf. Grounds Penetrating Radar, 2004. GPR 2004., 525–528, IEEE (2004).

[10] Eyuboglu, S., Mahdi, H., Al-Shukri, H. and Rock, L., "Detection of water leaks using ground penetrating radar," Proc. third Int. Conf. Appl. Geophys., 8–12, Orlando-FL (2003).

[11] Gamal, M., Di, Q., Zhang, J., Fu, C., Ebrahim, S. and El-Raouf, A. A., "Utilising ground-penetrating radar for water leak detection and pipe material characterisation in environmental studies: A case study," Remote Sens. **15**(20), 4924 (2023).

[12] Krapez, J.-C., Sanchis Muñoz, J., Mazel, C., Chatelard, C., Déliot, P., Frédéric, Y.-M., Barillot, P., Hélias, F., Barba Polo, J., Olichon, V., Serra, G., Brignolles, C., Carvalho, A., Carreira, D., Oliveira, A., Alves, E., Fortunato, A. B., Azevedo, A., Benetazzo, P., et al., "Multispectral Optical Remote Sensing for Water-Leak Detection," Sensors **22**(3), 1057 (2022).

[13] Arabi, S. and Grau, D., "Detecting underground water leaks with radar-multispectral fusion and machine learning," Remote Sens. Appl. Soc. Environ. **38**, 101594 (2025).

[14] Agapiou, A., Toulios, L., Themistocleous, K., Perdikou, S., Alexakis, D. D., Sarris, A., Toulios, G., Clayton, C. R. I., Phinikaridou, H., Manoli, A. and Hadjimitsis, D. G., "Use of satellite derived vegetation indices for the detection of water pipeline leakages in semi-arid areas," 5 August 2013, 879507.

[15] Mohsan, S. A. H., Khan, M. A., Noor, F., Ullah, I. and Alsharif, M. H., "Towards the unmanned aerial vehicles (UAVs): A comprehensive review," Drones **6**(6), 147 (2022).

[16] Theocharidis, C., Eliades, M., Kolokoussis, P., Miltiadou, M., Danezis, C., Gitas, I., Kontoes, C. and Hadjimitsis, D., "Exploring Sentinel-1 Radar Polarisation and Landsat Series Data to Detect Forest Disturbance from Dust Events: A Case Study of the Paphos Forest in Cyprus," Remote Sens. **17**(5), 876 (2025).

[17] Zhang, Y., Guan, H. and Duan, F., "Combined L-Band Polarimetric SAR and GPR Data to Develop Models for Leak Detection in the Water Pipeline Networks," Remote Sens. **17**(8), 1386 (2025).

[18] Yan, Y., Le, X., Yang, T. and Yu, H., "Interpretable PCA and SVM-based leak detection algorithm for identifying water leakage using SAR-derived moisture content and InSAR closure phase," IEEE J. Sel. Top. Appl. Earth Obs. Remote Sens. (2024).

[19] Mazzarotto, G., Tessari, G., Pizzaia, P. and Salandin, P., "Identifying pipeline leak positions potentially connected to soil deformations through SAR data analysis," J. Infrastruct. Syst. **29**(3), 4023017 (2023).

[20] Manataki, M., Papadopoulos, N., Sarris, A., Agapiou, A., Themistocleous, K. and Hadjimitsis, D. G., "Monitoring of water leakages from pipes through geophysical imaging methods," [Integrated Use of Space, Geophysical and Hyperspectral Technologies Intended for Monitoring Water Leakages in Water Supply Networks], InTech (2014).

[21] Hadjimitsis, D., Agapiou, A. and Themistocleous, K., [Integrated Use of Space, Geophysical and Hyperspectral Technologies Intended for Monitoring Water Leakages in Water Supply Networks], BoD–Books on Demand (2014).

[22] Hadjimitsis, D. G., Agapiou, A., Themistocleous, K., Toulios, G., Perdikou, S., Toulios, L. and Clayton, C., "Detection of water pipes and leakages in rural water supply networks using remote sensing techniques,"

[Remote sensing of environment-integrated approaches], IntechOpen (2013).
[23] Shen, Z., Yong, B., Gourley, J. J., Qi, W., Lu, D., Liu, J., Ren, L., Hong, Y. and Zhang, J., "Recent global performance of the Climate Hazards group Infrared Precipitation (CHIRP) with Stations (CHIRPS)," J. Hydrol. **591**, 125284 (2020).
[24] Zhao, Q., Yu, L., Li, X., Peng, D., Zhang, Y. and Gong, P., "Progress and trends in the application of Google Earth and Google Earth Engine," Remote Sens. **13**(18), 3778 (2021).
[25] Jin, S. and Sader, S. A., "Comparison of time series tasseled cap wetness and the normalised difference moisture index in detecting forest disturbances," Remote Sens. Environ. **94**(3), 364–372 (2005).
[26] Wang, L. and Qu, J. J., "NMDI: A normalised multi-band drought index for monitoring soil and vegetation moisture with satellite remote sensing," Geophys. Res. Lett. **34**(20) (2007).
[27] PBC, P. L., "Planet Insights Platform," 14 August 2024, <https://www.planet.com/products/planet-insights-platform/> (14 August 2025).
[28] Sitaropoulos, K., Salamone, S. and Sela, L., "Frequency-based leak signature investigation using acoustic sensors in urban water distribution networks," Adv. Eng. Informatics **55**, 101905 (2023).
[29] Almeida, F., Brennan, M., Joseph, P., Whitfield, S., Dray, S. and Paschoalini, A., "On the Acoustic Filtering of the Pipe and Sensor in a Buried Plastic Water Pipe and its Effect on Leak Detection: An Experimental Investigation," Sensors **14**(3), 5595–5610 (2014).
[30] Kadri, A., Abu-Dayya, A., Stefanelli, R. and Trinchero, D., "Characterisation of an acoustic wireless sensor for water leakage detection in underground pipes," 2013 1st Int. Conf. Commun. Signal Process. their Appl., 1–5, IEEE (2013).
[31] Lombardi, F., Podd, F. and Solla, M., "From Its Core to the Niche: Insights from GPR Applications," Remote Sens. **14**(13), 3033 (2022).
[32] Meng, X., Huang, Z., Deng, X., Liu, H., Fang, H., Liu, C., Zhang, X. and Cui, J., "Leakage detection and localisation of buried water pipe using ground penetrating radar," Measurement **254**, 117902 (2025).